The effect of polyelectrolyte on fabrication of macroporous ZrO$_2$ ceramics

YU JIA
National Institute of Advanced Industrial Science and Technology (AIST), Anagahora 2266-98, Shimoshidami, Moriyama-ku, Nagoya 463-8560, Japan

CIHANGIR DURAN
National Institute of Advanced Industrial Science and Technology (AIST), Anagahora 2266-98, Shimoshidami, Moriyama-ku, Nagoya 463-8560, Japan; Gebze Institute of Technology, Department of Materials Science and Engineering, P.K. 141, 41400, Gebze-Kocaeli, Turkey

YUJI HOTTA*, KIMIYASU SATO, KOJI WATARI
National Institute of Advanced Industrial Science and Technology (AIST), Anagahora 2266-98, Shimoshidami, Moriyama-ku, Nagoya 463-8560, Japan
E-mail: y-hotta@aist.go.jp

The effect of polyethylenimine (PEI) on preparing macroporous ZrO$_2$ materials via heterocoagulation coating process was investigated, using ZrO$_2$ nanoparticles as the building materials and polystyrene spheres as the organic templates. When PEI was applied to modify the surface charge of ZrO$_2$ nanoparticles, it was found that 40–50% of initial PEI amount remained excess in the suspensions. Adsorption of excess PEI on the surface of polystyrene spheres resulted in partial coating of the polystyrene spheres by ZrO$_2$ nanoparticles at 1 wt% PEI and even no coating at 3 wt% PEI. Microstructure studies revealed that ZrO$_2$ ceramics prepared without using PEI had quite ordered macropores, while the ZrO$_2$ framework was partially collapsed at 1 wt% PEI and disordered macropores were observed at 3 wt% PEI. © *2005 Springer Science + Business Media, Inc.*

1. Introduction

Well-ordered macroporous materials with three-dimensional periodicity are of significant interest in the last decades due to their potential applications in photonic crystals, catalysts, biomaterials and so on [1–5]. At present, various methods have been developed for preparing well-ordered macroporous materials. A colloidal crystal templating method using close-packed arrays of monodispersed template spheres (polystyrene or silica) was commonly applied to prepare three dimensionally ordered macroporous (3-DOM) materials such as silica [6, 7], metals [8–10], metal oxides [11–13], polymers [14] and carbon [15]. Nevertheless, control of wall thickness between pores was found to be limited. In addition to the crystal templating method, ordered macroporous materials with a controlled pore size were fabricated by a colloidal templating method using precoated templates [16–18]. A heterocoagulation method has also been applied to prepare well-ordered macroporous materials by utilizing commercial ceramic nanoparticles as building blocks [19–21]. The critical problem in this method is to prepare core and shell particles that are oppositely charged at the same pH range. There-fore, polyelectrolyte reagents have been frequently applied in order to modify the particle surface charge [19, 22–24].

In this study, the effect of polyethylenimine (PEI) on the fabrication of macroporous ZrO$_2$ ceramics was investigated. It was aimed to understand the role of PEI on heterocoagulation process between polystyrene spheres and nano ZrO$_2$ powders in aqueous suspensions. Characterization of the suspensions was carried out by zeta potential, particle size measurement and sedimentation kinetics. Green samples, prepared by slip casting, were used to analyze the microstructure of the macroporous materials sintered at 1000°C as a function of PEI content.

2. Experimental procedure

In the preparation of macroporous ZrO$_2$ materials, 3 mol% yttria-stabilized nano ZrO$_2$ powders (Aldrich, USA) with an average particle size of about 50 to 75 nm and specific surface area of 37.9 m^2/g were used as building blocks. As-received suspension of surfactant-free polystyrene spheres (PS) (8.2 wt%, average particle size of 1 μm, Interfacial Dynamics Corp.,

---

USA) was used as organic templates. Polyethylenimine (PEI) (MW 10000, Wako Pure Chemical Industries, Ltd., Japan) was applied to modify the ZrO_2 surface charges.

1 vol% ZrO_2 suspensions at various PEI contents were prepared by first dissolving PEI in distilled water and then adding ZrO_2 nanoparticles. Suspensions were ultrasonicated at 120 Watts for 10 min. Then, the suspensions were stirred for 6 h and finally centrifuged at 5000 rpm for 1 second. 5 ml PS suspension was dropped into 8 ml ZrO_2 suspension at various PEI contents during vigorous stirring and the resulting mixture was further stirred for 24 h. The suspensions prepared were as follows; (a) ZrO_2 suspensions containing 0 to 3 wt% PEI and (b) ZrO_2 suspensions containing 0 to 3 wt% PEI and PS templates. Pellets were formed by slip-casting, using gypsum molds. As-cast samples were dried at room temperature for 48 h and then fired at 1000°C for 2 h at a heating rate of 100°C/h.

The zeta potentials were measured using a laser electrophoresis analyzer (Model 502, Nihon Rufuto Co., Ltd, Japan). Reagent-grade HCl and NaOH were utilized to adjust pH to desired values. The particle size distribution was measured by a laser scatting particle size distribution analyzer (Horiba LA-920, Japan). A pulsed near infrared light was used to characterize sedimentation behavior of suspensions (Turbiscan ma 2000, Formulaction, France). Light transmitted and backscattered were recorded along the tube height as a function of time, which allowed suspension stability kinetics to be measured. A clarification region from the top and a sediment region at the bottom took place with time. In sedimentation kinetics analysis, depth of the clarification region from the top was considered and light transmitted at 3% intensity was used.

Amount of PEI adsorption was determined from Thermogravimetric Analysis (TG) (RTG320 Seiko Instruments, Japan). PEI-containing suspensions without PS were centrifuged at 25000 rpm for 15 min to separate sediment and supernatant. Sediment was washed with distilled water 2 times to remove free PEI. After final centrifugation, the sediment was dried at 100°C for 2 h before the TG analysis. TG of as-received ZrO_2 nanoparticles was chosen as a reference. Weight loss between 200–600°C was used in the adsorption calculations. Microstructure and pore morphology observations were performed by scanning electron microscopy (SEM) (Model JSM5600N, JEOL, Japan).

3. Results and discussion

Uniform coating of PS spheres with high surface area coverage requires that ZrO_2 particles be nano-scale as well as particle size distribution be narrow. However, mean particle size of as-received ZrO_2 nanoparticles was measured to be ~10 μm, which indicated that as-received nanoparticles were highly agglomerated. Therefore, a high-power ultrasonication at 120 W for 10 min was applied to deagglomerate the powders. Just after ultrasonication, mean particle size was

found to be 253 nm, with some particles as big as 1–3 μm. Suspension was lightly centrifuged at various speeds (1250, 3000 and 5000 rpm) for 1 second to separate bigger particles. It was found that the particle size was effectively decreased with increasing centrifugation speed. 10 min ultrasonication together with centrifuging at 5000 rpm for 1 sec resulted in a mean particle size of 114 nm with a very narrow particle size distribution. As a result of centrifuging, volume fraction of solid in the suspension was found to be 0.93 due to removal of bigger particles as sediment. These results indicate that both ultrasonication and centrifugation steps are necessary to prepare suspensions having finer particle size and narrower particle size distribution.

The zeta potential plots of PS and ZrO_2 nanoparticles prepared at various PEI contents are shown in Fig. 1. It is seen that ZrO_2 suspension with 0 wt% PEI has an isoelectric point (pH_{iep}) near 7. The pH_{iep} is increased with PEI addition, that is, it is ~9.2 at 1 wt% PEI and ~10.3 at 3 wt% PEI because PEI is a cationic polyelectrolyte [25]. On the other hand, the PS particles are negatively charged throughout the measured pH region due to the modification of sulfate functional groups. The pH of as-prepared ZrO_2 suspension with 0 wt% PEI was measured to be 4.6 and increased to 6.3 and 8.1 for suspensions with 1 and 3 wt% PEI, respectively. These pH values were remained the same after the nano ZrO_2 and PS suspensions were mixed. As is seen from Fig. 1, both building block nano ZrO_2 suspensions and organic template PS suspension are colloidally stable at the as-prepared pH conditions with opposite surface charges. Therefore, deposition of ZrO_2 nanoparticles on PS surfaces is expected due to electrostatic attraction on mixing of the two suspensions.

Fig. 2 shows the particle size distributions of nano ZrO_2, PEI-modified nano ZrO_2, PS and nano ZrO_2-coated PS particles. Mean particle sizes are also given. The plots indicate that all particle size distributions are unimodal. After 10 min ultrasonication and centrifugation at 5000 rpm for 1 s, all of the dispersed ZrO_2 nanoparticles modified with different contents of PEI (0 to 3 wt%) have a mean particle size around 115 to130 nm with a very narrow particle size distribution
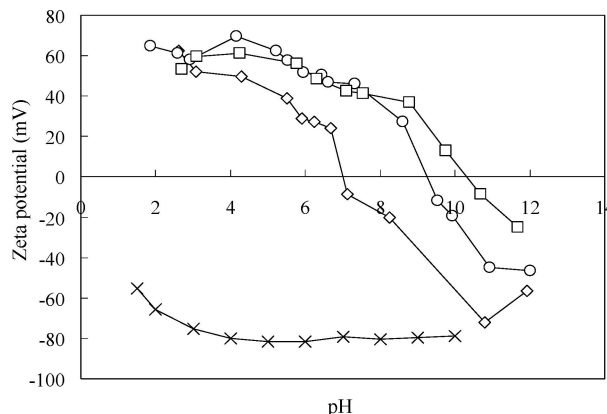

Figure 1 Zeta potential plots of PS particles ($\times$) and ZrO_2 nanoparticles with ($\diamond$) 0 wt% PEI, ($\circ$) 1 wt% PEI and ($\square$) 3 wt% PEI.
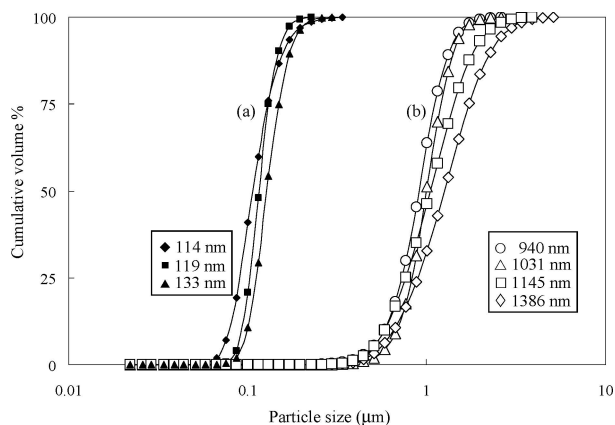
Figure 2 Particle size distributions as a function of PEI content; (a) ZrO$_2$ nanoparticles with: (◆) 0 wt% PEI, (■) 1 wt% PEI and (▲) 3wt% PEI, and (b) nano ZrO$_2$-coated PS particles with: (◇) 0 wt% PEI, (□) 1 wt% PEI, and (△) 3 wt% PEI. Size distribution of PS particles is given for comparison (○).

(Fig. 2a), which indicates that ultrasonication and centrifugation method was quite effective for deagglomeration of the ZrO$_2$ nanoparticles and removal of the bigger particles. The SEM micrographs (not shown here) also indicated that the as-prepared ZrO$_2$ suspensions were agglomeration-free. The mean particle size of PS particles was measured to be 940 nm, while nano ZrO$_2$-coated PS particles had a mean particle size of 1386, 1145 and 1031 nm at 0, 1 and 3 wt% PEI contents, re-

spectively (Fig. 2b). The coated PS particles at 0 wt% PEI have a mean particle size bigger than the theoretical single layer coverage of ZrO$_2$ nanoparticles, which may result from a slight flocculation of the coated particles. The coated PS particles at 1 wt% PEI have a smaller particle size, which indicates a partial coating, whereas the one at 3 wt% PEI has no apparent increase in size as compared to the raw PS particles, which suggests that the deposition of ZrO$_2$ nanoparticles on PS surface did not take place.

Fig. 3 shows SEM images of PS and nano ZrO$_2$-coated PS particles. The SEM micrographs of the PS (Fig. 3a) and nano ZrO$_2$ (0 wt% PEI) coated PS particles (Fig. 3b) reveal that an effective surface coverage of PS particles with ZrO$_2$ nanoparticles took place successfully after mixing, as clearly evident from rough surfaces of each PS particle compared to the smooth surfaces of the uncoated PS particles. Only partially coated particles are observed at 1 wt% PEI content (Fig. 3c), whereas deposition of nano ZrO$_2$ on PS surface is almost nil at 3 wt% PEI content (Fig. 3d). In addition, ZrO$_2$ nanoparticles are present in the latter as free powders filling the voids. The SEM observation agrees well with the particle size distribution results (Fig. 2) in that when PEI is applied, surface coverage of PS particles with ZrO$_2$ nanoparticles consistently decreases.

Fig. 4 shows the sedimentation behaviors of the mixtures of ZrO$_2$ and PS suspensions. The plots indicate advance of clarification depth from the suspension top
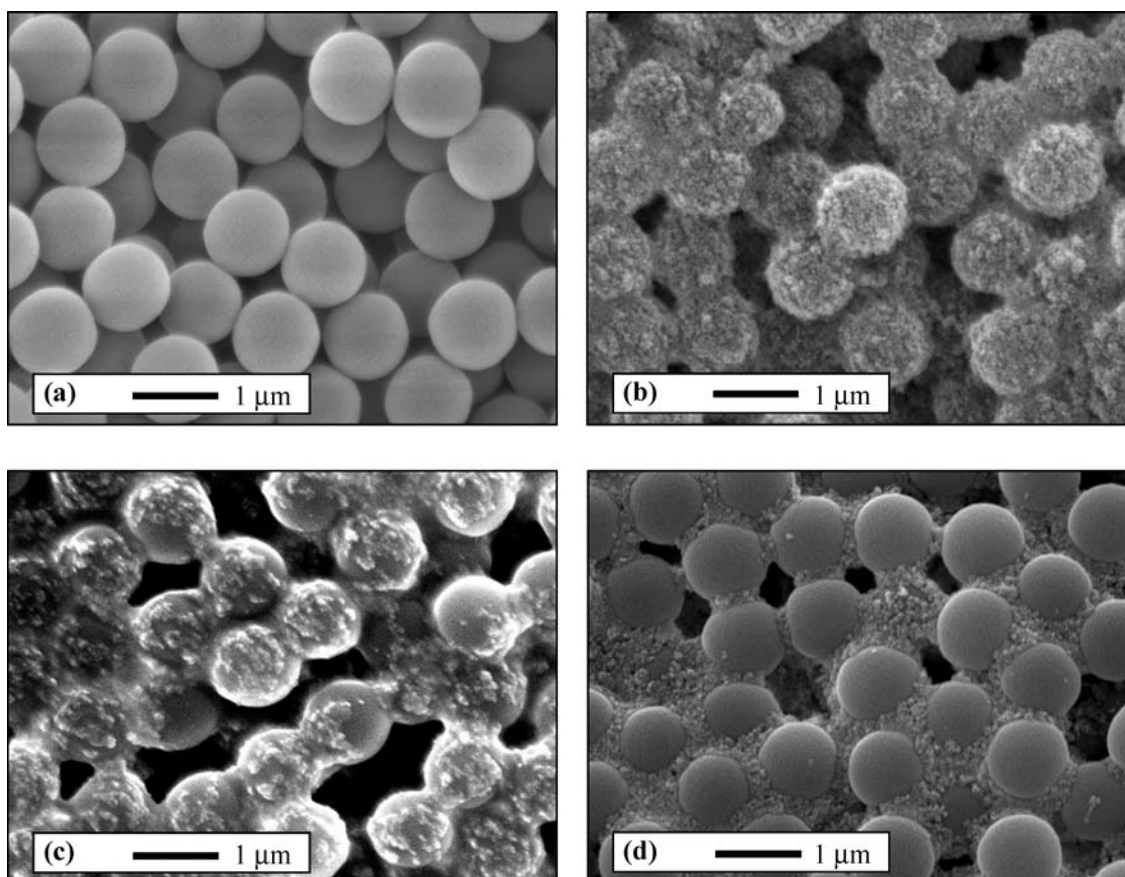

Figure 3 SEM micrographs of (a) as-received PS particles and nano ZrO$_2$-coated PS particles with; (b) 0 wt% PEI, (c) 1 wt% PEI, and (d) 3 wt% PEI.
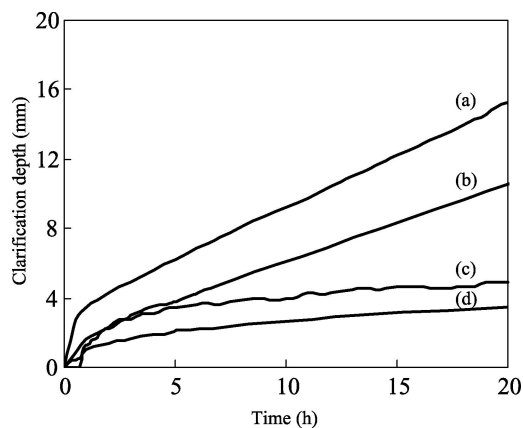
Figure 4 Sedimentation kinetics of mixtures prepared from PS and nano ZrO₂ suspensions as a function of PEI content; (a) 0 wt% PEI, (b) 1 wt% PEI, (c) 3 wt% PEI. Sedimentation kinetics of PS suspension is given for comparison (d).

Figure 6 Amount of PEI adsorbed as a function of initial amount of PEI.

as a function of time. The sedimentation kinetic data reveals that the mixtures of ZrO₂ and PS suspensions have different sedimentation behaviors depending on the PEI contents, with a trend approaching to that of original PS suspension with increasing PEI content. Suspension with 0 wt% PEI has an average rate of 0.61 mm/h as compared to 0.45 mm/h at 1 wt% PEI content and 0.23 mm/h at 3 wt% PEI content. The rate at 3 wt% PEI content is quite similar to that of PS particles (0.22 mm/h). Note that the sedimentation rate is given as average rate, which is calculated from linear sections of each curve. The sedimentation rate of the suspensions, especially at 0 wt% and 1 wt% PEI, is a little bit faster in the first several hours, which results from the sedimentation of flocculated particles. The sedimentation results are in good agreement with the particle size (Fig. 2) and SEM (Fig. 3) results in that the particle size increases with decreasing PEI content due to the efficient coverage of PS surfaces with ZrO₂ nanoparticles.

Fig. 5 shows zeta potential plots of nano ZrO₂-coated PS particles. It can be observed that the zeta potential plots of the coated particles are very similar to those given in Fig. 1 for the ZrO₂ nanoparticles. Not only full
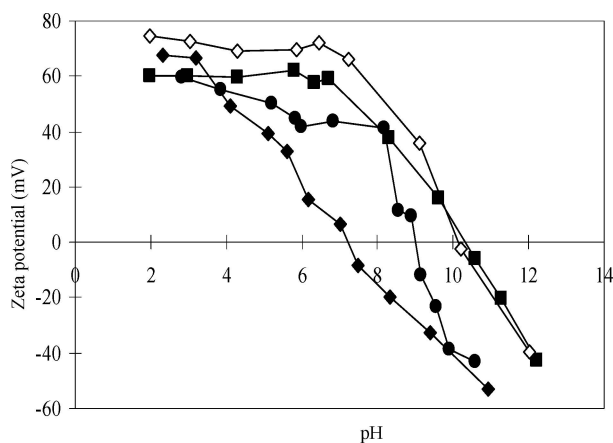
coverage at 0 wt% PEI and partial coverage at 1 wt% PEI, but also no coverage at 3 wt% PEI did change the surface charge of the PS particles in the suspensions. Fig. 5 also shows the zeta potential of PS particles after mixing with the supernatant of 3 wt% PEI-added ZrO₂ suspension. Change of the surface charge of PS particles without ZrO₂ coating can be attributed to the presence of excess PEI in the as-prepared ZrO₂ suspension. Fig. 6 shows the amount of PEI adsorbed on ZrO₂ nanoparticles as a function of initial PEI contents as determined from the TG analysis. It indicates that there were some excess PEI remained in the suspension. Nearly 52% excess PEI (about 0.25 wt% with respect to dry weight of PS) remained in the suspension at 1 wt% PEI. When the initial PEI content was further increased to 3 wt%, there was 42% excess PEI (about 0.61 wt% with respect to dry weight of PS) remained in the suspension. After ZrO₂ and PS suspensions were mixed, the positively charged excess PEI easily adsorbed on the surface of negatively charged PS particles by electrostatic attraction, which, in turn, gave rise to modification of the surface potential of PS particles. From the zeta potential plot of the PS particles after mixing with the supernatant of ZrO₂ suspension with 3 wt% PEI (Fig. 5), it is seen that the zeta potential of PS particles is shifted from negative to positive below pH ∼ 10, which confirms the adsorption of excess PEI on PS particles. The TG analysis and zeta potential results are parallel to SEM (Fig. 3), particle size distribution (Fig. 2) and sedimentation (Fig. 4) results in regard to the effect of excess PEI on coating efficiency.

Fig. 7 shows the SEM micrographs obtained from as-sintered surface of the samples prepared at different PEI contents and sintered at 1000°C for 2 h. Closely packed and uniformly distributed pores are observed in the sample with 0 wt% PEI after the PS templates were burn out, which can be attributed to uniform and high surface area coating of PS particles (Fig. 7a). However, some broken walls between pores are observed when the PEI content is 1 wt% (Fig. 7b). Furthermore, the microstructure of the sample with 3 wt% PEI consisted of dispersed macropores and separately sintered

Figure 5 Zeta potential plots of nano ZrO₂-coated PS particles with; (◆) 0 wt% PEI, (●) 1 wt% PEI, and (■) 3 wt% PEI. The plot of PS particles after mixing with the supernatant of 3 wt% PEI-added ZrO₂ suspension is also given (◇).
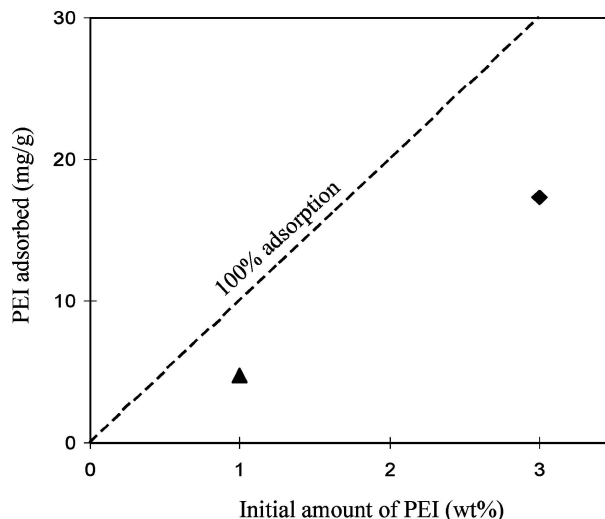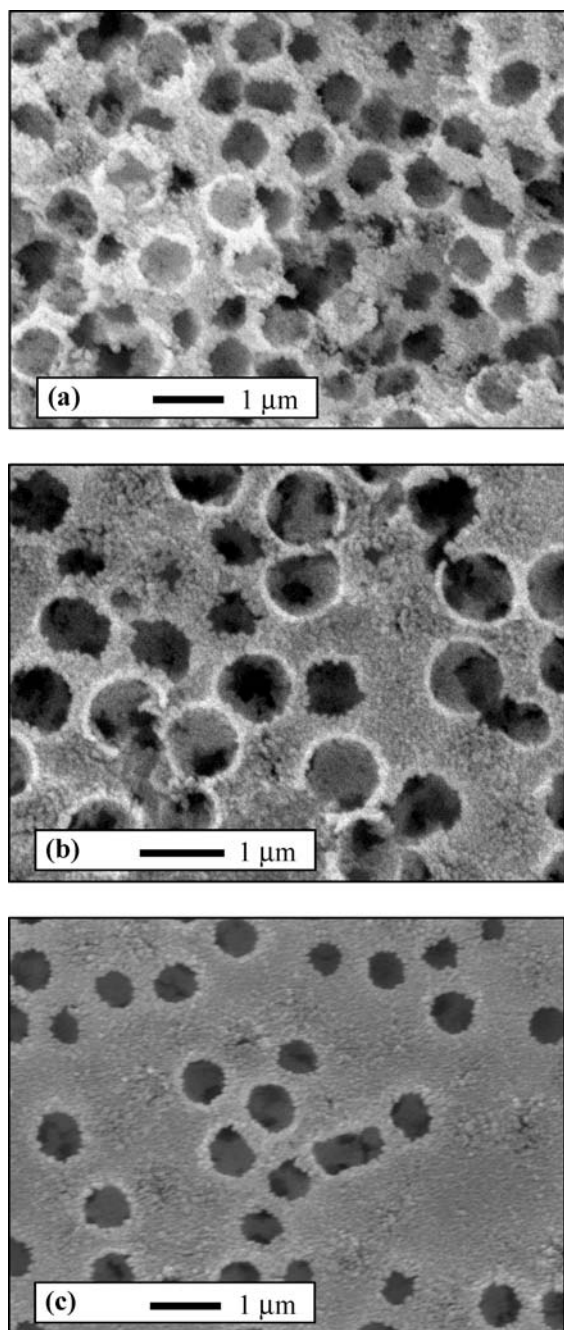
Figure 7 SEM micrographs from as-sintered surfaces of samples with; (a) 0 wt% PEI, (b) 1 wt% PEI, and (c) 3 wt% PEI. Samples were sintered at 1000°C for 2 h.

ZrO_2 nanoparticles (Fig. 7c). Effect of sintering temperature on macroporous ZrO_2 ceramics was described elsewhere [21].

It was mentioned so far that excess PEI has a profound effect on efficient coating of PS particles with ZrO_2 nanoparticles. The coating and forming processes at different PEI contents are schematically described in Fig. 8. The numbers I, II, and III represent respective suspensions. At the beginning (Fig. 8a), each suspension (e.g., ZrO_2, PS, and PEI-added ZrO_2) is highly stable. At 0 wt% PEI, the PS particles are fully covered with ZrO_2 nanoparticles. Besides, the mixed suspension has a high stability due to the high surface charge of ZrO_2 nanoparticles (Fig. 5). However, particle size distribution is slightly broader at 0 wt% PEI content (Fig. 2b). The possible reason could be the bridg-

ing of negatively charged PS particles by positively charged ZrO_2 nanoparticles during mixing (shown as letter *A* in Fig. 8b), which results in a slight flocculation of PS particles. The sedimentation rate, in fact, is higher in the first couple hours of the test (Fig. 4a), proving some degree of flocculation. However, well-ordered macroporous ceramic can be prepared after sintering in the absence of PEI (Fig. 7a). As for the suspensions containing PEI, excess PEI adsorbed on PS particles hinders an effective coverage of PS particles with ZrO_2 nanoparticles. The adsorption of excess PEI modifies the surface potential of PS particles from negative to positive (Fig. 5), which, in fact, effectively prevents further deposition of ZrO_2 nanoparticles by means of electrostatic repulsion. At 1 wt% PEI, partial coating takes place because excess PEI amount is less (e.g., 0.25 wt% with respect to the PS amount). Local flocculation of PS particles is caused by excess, positively charged PEI (shown as letter *B* in Fig. 8b). In this case, flocculated PS particles without adherence of nano ZrO_2 building block results in the collapse of the framework locally after the organic templates were burn out. When PEI amount is further increased to 3 wt%, too much excess PEI remains in the suspension (e.g., 0.61 wt% with respect to the PS amount) and almost all PS particles are modified with PEI. By this way, coating of PS particles with ZrO_2 nanoparticles is almost totally eliminated, as also seen in Fig. 3d. However, the mixed suspension is well-dispersed because both nano ZrO_2 and PS particles are positively charged (Fig. 5). Furthermore, some of the PS particles easily connect without the building block ZrO_2 nanoparticles during the slip casting process. Therefore, the pores are randomly distributed in the sintered structure.

These results clearly suggest that PEI should not be added at all at fabricating macroporous ZrO_2 materials if one desires to have a well-ordered, self-supporting structure. If PEI is to be used, however, it is highly recommended that excess PEI must be removed (e.g., by washing ZrO_2 nanoparticles in a way similar to the TG sample preparation described in Section 2) before ZrO_2 building block and organic polystyrene template suspensions are mixed. Removing excess polyelectrolyte is quite important when the use of polyelectrolyte becomes a must for some ceramic systems where species dissolution is inevitable due to suspension pH. For example, Ba^{2+} dissolution in aqueous $BaTiO_3$ suspension is favored towards the acidic region, resulting in an isoelectric point near pH 4.5 due to the formation of TiO_2-rich surface layer on $BaTiO_3$ [26]. It was reported that Ba^{2+} dissolution can be prevented towards the alkaline region (e.g., after pH 8) [27]. Therefore, if one wants to fabricate macroporous $BaTiO_3$ ceramics using PS templates, isoelectric point must be modified towards the alkaline region both to prevent Ba^{2+} dissolution and to induce positive surface charge for heterocoagulation process, using polyelectrolyte. In this work, it was shown an example for ZrO_2-polystrene-PEI-water system, but choice has to be made depending on the ceramic-organic template-polyelectrolyte-solvent system.
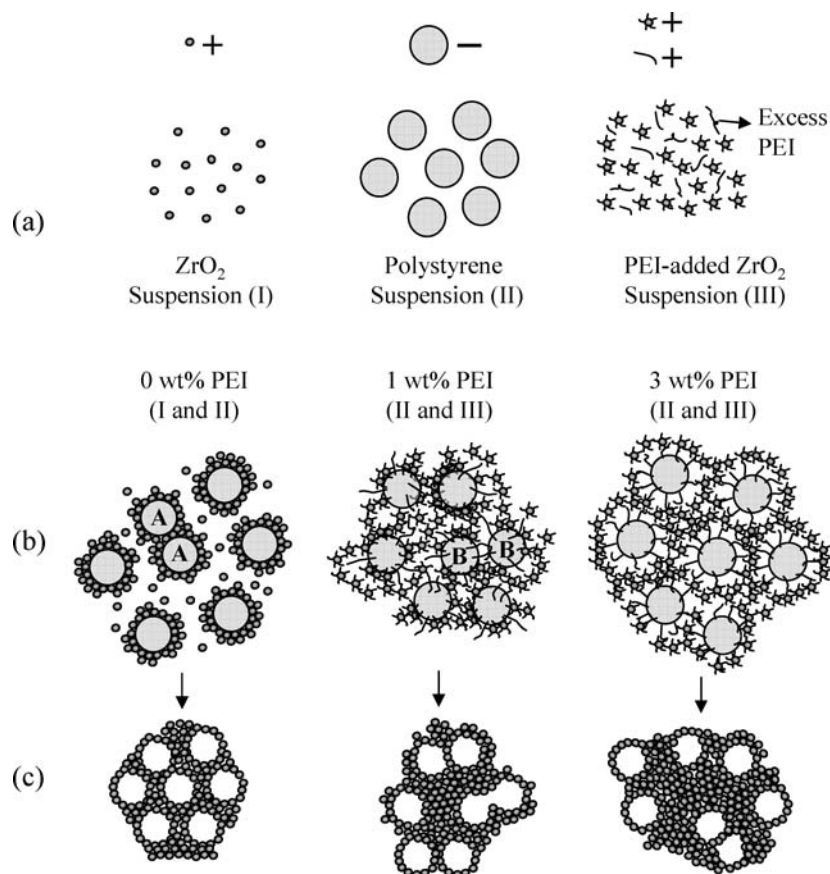
Figure 8 Schematic views of macroporous ZrO_2 fabrication; (a) individual suspensions, (b) mixed suspensions, and (c) microstructure after heat treatment. Surface charges pertaining to ZrO_2, PS, PEI, and PEI-added ZrO_2 are shown at the top.

4. Conclusions

This work was focused on the effect of polyethylenimine (PEI) on preparation of well-ordered macroporous ZrO_2 materials, derived from ZrO_2 nanoparticles as the building block materials and polystyrene spheres as the organic templates. ZrO_2 nanoparticles containing 0 to 3 wt% PEI had a mean particle size around 115 to 130 nm with a very narrow particle size distribution. TG results showed that about 40–50% of initial PEI amount remained excess in the suspensions. After the heterocoagulation process, the mean particle size of nano ZrO_2-coated PS particles without PEI was found to be 1386 nm, as compared to 1145 nm at 1 wt% PEI and 1031 nm at 3 wt% PEI addition, indicating that surface coverage of PS particles with ZrO_2 nanoparticles consistently decreased in the presence of PEI because excess PEI modified the PS surface charge from negative to positive which resulted in an electrostatic repulsion between nano ZrO_2 and PS particles. Microstructure studies indicated that ZrO_2 ceramics with well-ordered macropores could be prepared without applying PEI, whereas partially collapsed ZrO_2 framework at 1 wt% PEI and disordered macropores at 3 wt% PEI were obtained. Therefore, PEI should not be added at all at fabricating macroporous ZrO_2 materials if one desires to have a well-ordered and self-supporting structure. If PEI is to be used, however, excess PEI must be removed before nano ZrO_2 building block and organic polystyrene template suspensions are mixed.

References

1. M. HAROLD, C. LEE, A. J. BURGGRAAF, K. KEIZER, V. T. ZASPALLS and R. S. A. DE LANGE, *Mater. Res. Soc. Bull.* **19** (1994) 34.
2. K. ISHIZAKI, S. KOMARNENI and M. NAUKO, "Porous Materials Process Technology and Applications" (Kluwer, London, UK 1998).
3. S. F. CORBIN and P. S. APTE, *J. Am. Ceram. Soc.* **82** (1999) 693.
4. J. E. G. J. WIJMHOVEN and W. L. VOS, *Science* **281** (1998) 802.
5. G. T. CHANDRAPPA, N. STEUNOU and J. LIVAGE, *Nature* **416** (2002) 702.
6. O. D. VELEV. T. A. JEDE, R. F. LODO and A. M. LENHOFF, *ibid.* **389** (1997) 447.
7. B. T. HOLLAND, L. ABRAMS and A. STERN, *Chem. Mater.* **11** (1999) 795.
8. H. YAN, C. F. BLANFORD, B. T. HOLL, M. PARENT, W. H. SMYRL and A. STEIN, *Adv. Mater.* **11** (1999) 1003.
9. P. JIANG, J. CIZERON, J. F. BERTONE and V. L. COLVIN, *J. Am. Chem. Soc.* **121** (1999) 7957.
10. O. D. VELEV, P. M. TESSIER, A. M. LENHOFF and E. W. KALER, *Nature* **401** (1999) 548.
11. S. SOKOLOV, D. BELL and A. STEIN, *J. Am. Ceram. Soc.* **86** (2003) 1481.
12. D. WANG, R. A. CARUSO and F. CARUSO, *Chem. Mater.* **13** (2001) 364.
13. H. YAN, C. F. BLANFORD, B. T. HOLLAND, W. H. SMYRL and A. STEIN, *ibid.* **12** (2000) 1134.
14. S. H. PARK and Y. XIA, *ibid.* **10** (1998) 1745.
15. A. A. ZAKHIDOV, R. H. BAUGHMAN, Z. IQBAL, C. CUI, I. KHAYRULLIN, S. O. DANTAS, J. MARTI and V. G. RALCHENKO, *Science* **282** (1998) 897.
16. F. CARUSO and H. MÖHWALD, *Langmuir* **15** (1999) 8276.
17. Y. HOTTA, P. C. A. ALBERIUS and L. BERGSTRÖM, *J. Mater. Chem.* **13** (2003) 496.

18. K. H. RHODES, S. A. DAVIS, F. CARUSE, B. ZHANG and S. MANN, *Chem. Mater.* **12** (2000) 2832.
19. F. Q. TANG, H. FUDOUZI and Y. SAKKA, *J. Am. Ceram. Soc.* **86** (2003) 2050.
20. N. S. SANJANI, N. NADERI and M. S. DEHGHAN, *Mater. Sci. Forum.* **437** (2003) 419.
21. Y. JIA, C. DURAN, Y. HOTTA, K. SATO and K. WATARI, submitted to *J. Coll. Inter. Sci.* (2004).
22. T. GARINO, *J. Am. Ceram. Soc.* **75** (1992) 511.
23. E. ZHAO, S. E. HARDCASTLE, G. PACHECO, A. GARCOA, A. L. BLUMENFELD and J. J. FRIPIAT, *Micropor. Mesopor. Mater.* **31** (1999) 9.
24. Z. LIANG, A. S. SUSHA, A. YU and F. CAROUS, *Adv. Mater.* **15** (2003) 1849.
25. J. WANG and L. GAO, *Nanostr. Mater.* **11** (1999) 451.
26. W.-H. SHIH, D. KISAILUS and Y. WEI, *Mater. Lett.* **24** (1995) 13.
27. Z.-G. SHEN, J.-F. CHEN, H.-K. ZOU and J. YUN, *J. Coll. Inter. Sci.* **275** (2004) 158.